 doi:10.20944/preprints202209.0023.v1

Article

Mathematical model of pancreatic cancer cell dynamics considering the set of sequential mutations and interaction with the immune system

Alexander S. Bratus[1,2], Nicholas Leslie[3], Michail Chamo[1], Dmitry Grebennikov[4,5,6], Rostislav Savinkov[4,5,6], Gennady Bocharov[4,5,6] and Daniil Yurchenko[7]

1 Russian University of Transport, Moscow, Russian Federation; alexander.bratus@yandex.ru(A.B.)
2 Moscow Center for Fundamental and Applied Mathematics at Lomonosov Moscow State University, Moscow, Russian Federation
3 Heriot-Watt University, Edinburgh, United Kingdom
4 Marchuk Institute of Numerical Mathematics, Russian Academy of Sciences, Moscow, Russian Federation
5 Moscow Center for Fundamental and Applied Mathematics at INM RAS, Moscow, Russian Federation
6 Sechenov First Moscow State Medical University, Moscow, Russian Federation
7 University of Southampton, Highfield, Southampton, United Kingdom
* Correspondence: alexander.bratus@yandex.ru; (A.B.)

Abstract: Pancreatic cancer represents one of the difficult problems of contemporary medicine. The development illness evolves very slowly, takes place in special sake (stroma) and manifests clinically close to a final stage. Another feature of this pathology is a coexistence (symbiotic) effect between cancer cells and normal cells inside stroma. All these aspects make it difficult to understand the pathogenesis of pancreatic cancer and develop a proper therapy. The emergence of pancreatic pre-cancer and cancer cells represents a branching stochastic process engaging populations of 64 cells differing in the number of acquired mutations. In this study we formulate and calibrate the mathematical model of pancreatic cancer using the quasispecies framework. The mathematical model incorporates the mutation matrix, fineness landscape matrix and the death rates. Each element of the mutation matrix presents the probability of appearing a specific mutation in the branching sequence of cells representing the accumulation of mutations. The model incorporates the cancer cell elimination by effect CD8 T cells (CTL). The down-regulation of the effector function of CTLs and exhaustion are parameterized. The symbiotic effect of coexistence of normal and cancer cells is considered. The computational predictions obtained with the model are consistent with empirical data. The modelling approach can be used to investigate other types of cancers and examine various treatment procedures.

Keywords: Pancreatic cancer; cancer evolution; tumour microenvironment; mathematical model; open quasispecies model

Citation: Lastname, F.; Lastname, F.; Lastname, F. Title. *Preprints* **2022**, *1*, 0. https://doi.org/

1. Introduction

Pancreatic cancer has the worst prognosis of all major cancer types, with very poor treatment options. Less than 10% of patients will live for more than five years after diagnosis [1,2]. The main reasons for this are as follows.

1. The process of formation of precancerous and cancerous cells represents a successive chain of mutations over a relatively long period of time (10 to 20 years). During this time, the disease often causes very limited noticeable symptoms and the cancer has often already spread at the time of diagnosis, with the most common sites of metastasis being the liver, lung and peritoneum [3].
2. Pancreatic tumours are comprised of cancer cells surrounded by other cell types and extracellular matrix, collectively known as the tumour stroma. The dense stroma of pancreatic cancer makes both diagnosis and treatment more difficult [4,5].
3. A favorable microenvironment for tumour progression exists inside the stroma, built in large part upon symbiotic interactions between non-cancerous pancreatic cells and precancerous and cancerous cells. [4,6–9].

 doi:10.20944/preprints202209.0023.v1

4. The genetic changes which drive pancreatic cancer do not reveal any clear vulnerabilities to available therapies and the success with existing treatments is very limited [1,10].

Surgery before the disease has spread remains the only treatment likely to be curative, however, <15% of patients are selected for surgery and there are no broadly used methods for identifying patients at this early potentially curable stage. The most common treatment for metastatic or locally advanced pancreatic cancer are aggressive chemotherapies which modestly extend survival and to date targeted therapies have provided little or no benefit [1]. Approximately 85% of pancreatic cancers are defined as Pancreatic Ductal AdenoCarcinoma (PDAC) and many, perhaps most, of these tumours are believed to develop from precursor lesions termed Pancreatic Intraepithelial Neoplasia (PanIN) [11]. However, the sequences of genetic changes which lead to PDAC and the consequences of these evolutionary processes on the responses to therapy remain unclear [12,13]. Initial models proposed sequential events in key drivers over many years: activating mutation of a copy of KRAS, followed by bi-allelic loss of CDKN2A, TP53 and SMAD4 [14]. However, more recent data imply that multiple loss of function events may occur simultaneously [15].

Therefore, to deepen our understanding of these processes and to derive testable predictions, we elected to develop a mathematical model of PDAC progression. This describes the dynamics of species communities, taking mutations into account, M. Eigen's replicator system of quasispecies [16].

1.1. Framework for quasispecies dynamics

In this study, the quasispecies term implies the set of distinct cell populations (species) which differ with respect to the acquired genetic mutations. The respective mathematical model represents an ODE system describing the evolution of population frequencies, taking into account the set of possible mutations:

$$\frac{dp(t)}{dt} = (QM)p(t) - p(t)f(p) \tag{1}$$

where $p = (p_1, p_2, ..., p_n)$ is a vector of frequencies (relative numbers of species). Note that in the classical theory of quasispecies the total number of species remains constant at $t \geq 0$. Matrix $Q = (q_{ij}), \quad i, j = 1, 2, ..., n$ represent the probability of mutations, i.e. q_{ij} sets the probabilities that replicating a species with index j results in a species with number i:

$$\sum_{i=1}^{n} q_{ij} = 1, \quad j = 1, 2, ..., n \tag{2}$$

The diagonal matrix $M = diag(m_1, m_2, ..., m_n)$ defines the viral fitness landscape. In other words, each species is assigned a number that characterises its ability to survive in the system. Usually the fitness landscape is quantified on the basis of species growth rates and other data on the dominant properties of the species. The system of quasispecies dynamics describes the evolution of species communities, taking into account possible mutations, but ignoring the natural mortality rates of species. In order to account for species mortality, a modified (open) quasispecies system [16] was proposed, in which the total number of species is not a constant value. Let $u_i(t)$ be the abundance of species i, $t \geq 0$, M and Q the species adaptation matrix and mutation matrix respectively.

Let us introduce the following function

$$S(u) = \sum_{i=1}^{n} u_i(t) = 1. \tag{3}$$

The function $S(u)$ defines the total number of species at time $t \geq 0$. The function $\Phi(s)$ is characterized by the following properties:

(a) $\Phi(s)$ is a smooth function $s \in [0, c), \quad c \geq 0$;

 doi:10.20944/preprints202209.0023.v1

(b) $\Phi(s) > 0, \quad s \in [0, c)$;
(c) If $0 < c < +\infty$, then $\lim_{s \to c} s\Phi(s) = 0$;
(d) Function $s\Phi(s) = 0$ has only one maximum at the point s^*, $0 < c < c^*$.

As an example of function $\Phi(s)$, we can consider the functions $\Phi(s) = (c - s),\ c > 0,\ 0 < s < c$ or $\Phi(s) = \exp(-\gamma s), \gamma > 0, s > 0$.

Consider the diagonal matrix describing species mortality rates $D = diag(d_1, d_2, ..., d_n)$. Let the elements of the fitness landscape matrix M and the mortality matrix satisfy the following conditions

$$\begin{aligned} &0 \le m_{min} \le m_i \le m_{max} \\ &0 \le d_{min} \le d_i \le d_{max}, \quad i = 1, 2, ..., n \\ &0 < d_{max} < m_{min}. \end{aligned} \tag{4}$$

Here are the model equations describing the population dynamics of species:

$$\begin{aligned} &\frac{du(t)}{dt} = \Phi(s)(QM)u(t) - Du(t) \\ &u(0) = u^0 \ge 0 \end{aligned} \tag{5}$$

System (5) is positively invariant for any non-negative initial conditions $u(0) \ge 0$. There exists a unique solution to this problem. When conditions (4) are satisfied, the total number of species (3) as well as the species abundances are bounded functions on the system trajectories [16]. The average fitness of open system (5) is defined by

$$f(u) = \begin{cases} 0, & s(u) = 0 \\ \frac{\sum_{i=1}^{n} m_i u_i(t)}{\sum_{i=1}^{n} d_i u_i(t)} = (\Phi(s))^{-1}, & s(u) \ne 0 \end{cases} \tag{6}$$

where, the numerator of the expression is equal to the average fitness of quasispecies (1), and the denominator reflects the decline of the species community due to their mortality.

In section 2, the mutational pathways of the normal cells are characterized. In section 3, the mathematical model of tumor-immune cell dynamics if developed. The results of numerical simulations are presented in section 4. The results are briefly discussed in Conclusion section.

2. Development of the cancer mutations

The vast majority (>85%) of Pancreatic Cancers are defined as Pancreatic Ductal Adenocarcinomas are driven by activating mutations in a single copy of the KRAS gene (85-95%) and also displaying very frequent loss of function mutations in TP53 (>75%), CDKN2A (>30-60%) and SMAD4 (30-50%). Here, these mutations have been abbreviated as K, P, C and S mutations respectively. Figure 1 represents the chain of successive mutations of growing pancreatic cancer cell populations. Healthy cells (N) with the potential for oncogenic transformation to PDAC [17,18] are characterised by a high probability of slow error-free replication $p_0 = 0.999999$. Each healthy originating cell can proliferate or die, according to data presented in Table 1, whereas at any given time most of them are non-replicative. Table 1 summarizes the doubling time data for different cell types, as well as data on type mortality rates.

Preprints (www.preprints.org) | NOT PEER-REVIEWED | Posted: 1 September 2022 doi:10.20944/preprints202209.0023.v1

Table 1. Data on doubling times and mortality rates for cell types bearing specific mutations.

Mutation type	Doubling time (days)	Mortality
K (KRAS)	200	3.22%
P (TP53)	800	0.86%
C (CDKN2A)	800	1%
S (SMAD4)	1	0.9%
KC	140	15%
KS	180	20%
KP	180	8%
PS	750	5%
CP	600	5%
CS	600	5%
KCS	120	20%
KPC	120	10%
KPS	120	10%
CPS	500	5%
$KPCS$	100	8%

With probability of $p_m \approx 10^{-7}/4$ per cell per generation, healthy cells will be subject to an activating mutation in a single allele of KRAS. Similarly, we estimate the probability of loss of function mutations in the second copy of CDKN2A (C), TP53 (P) or SMAD4 (S) to be $10^{-7}/4$ per cell per generation. For simplicity it is assumed that loss of the first copy of these tumour suppressors has no effect on cell fitness. Therefore, healthy N cells are converted with the probability p leading to K, P, C or S mutant cells, as shown in Figure 1.

These initiating mutations in key genes, K, C, P and S would be expected in many cases to lead to Oncogene Induced Senescence . Therefore, the loss from the model of these cells upon mutation is defined by probability p_{d_i}. Otherwise, the mutant cells of K type, as demonstrated in Figure 1, can proliferate and die as K-mutants with probabilities shown in Table 1, but can also give a new mutation of P, C or S type, resulting in KP, KC or KS double-mutants correspondingly. At this and consequent stages after adaptation, the new mutants are believed to avoid oncogene induced senescence. These double-mutants can also proliferate, die or give a rise to triple-mutant cells, i.e. KPS, KPC, KCP, KCS, etc, as shown in Figure 1.

As a result, the overall number of mutated cells is 64. To continue, it is important to enumerate all cell types. The continuous numbering is introduced starting from a single-mutant cells as illustrated in Table 2 and Figure 1. Overall, the one-letter cells correspond to numbers from 1 to 4, two-letter cells — from 5 to 16, three-letter cells — from 17 to 40, four-letter cells — from 41 to 64.

Table 2. An illustration of the enumeration rule for the one-letter and two-letter designated types of mutated cells.

Cell type	K	P	C	S	KP	KC	KS	PK
Number	1	2	3	4	5	6	7	8
Cell Type	PC	PS	CK	CP	CS	SK	SP	SC
Number	9	10	11	12	13	14	15	16

Healthy cells mutate into one-letter type with probability $q_0 = p = \frac{1}{4}10^{-7}$. Given the assumptions stated above, the probabilities of one-letter type mutations are $q_1 = pp_1(1 - p_d)$.

Next, we assume that the probabilities of the mutations converting cells with a single mutation into cells carrying two mutations (i.e., one-letter cell types to the two-letter cell

Preprints (www.preprints.org) | NOT PEER-REVIEWED | Posted: 1 September 2022 doi:10.20944/preprints202209.0023.v1

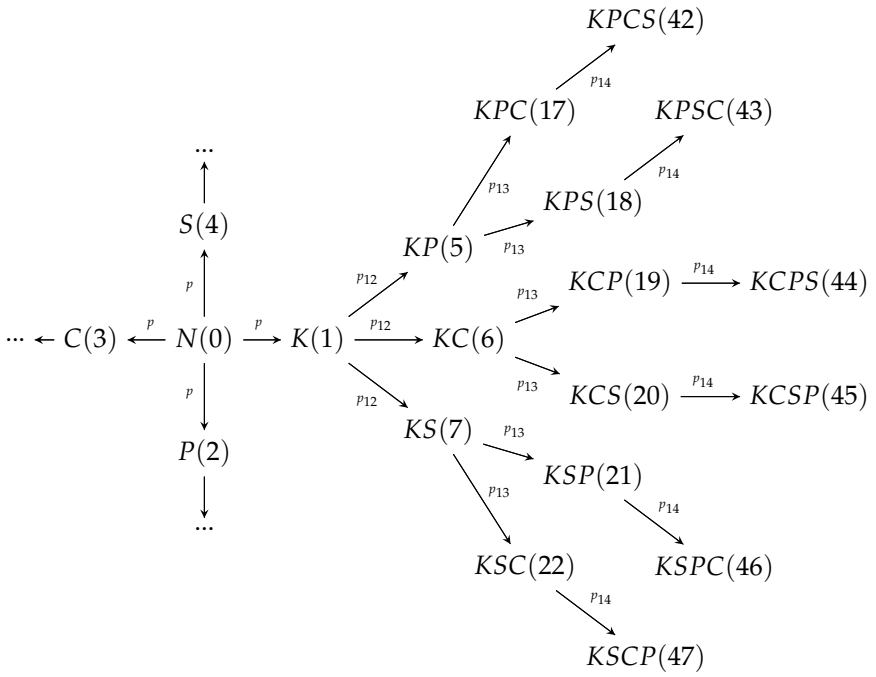

Figure 1. Scheme illustrating the evolution of possible mutations of healthy cell N. The branch following the initial mutation K is shown in detail. For clarity, the evolutionary schemes evolving from the alternative initial P(2), C(3) and S(4) mutations are not included within the diagram.

types) and the subsequent mutations of these cells into the three-letter and four-letter cell types are identical:

$$p_{m1} = p_1 = \frac{1}{12}, \quad p_{m2} = p_{m3} = p_{m4} = p_2 = \frac{1}{24}.$$

Probabilities of two-letter type mutations are:

$$q_2 = pp_1^2(1 - p_d)^2 \tag{7}$$

Accordingly, three-letter and four-letter:

$$q_3 = pp_1^3(1 - p_d)^3 \tag{8}$$

$$q_4 = pp_1^4(1 - p_d)^4 \tag{9}$$

Unfortunately, data on the probability of instantaneous mortality of p_d species are unknown to us. All subsequent calculations will be made using $p_d = 0.5$.

Fitness rates m_i and death rates d_i in the stated order of cell type enumeration are presented on Figure 2. Based on the data in Table 1, we construct a matrix M that defines the fitness landscape of species. Let's take 1200 days as a unit of fitness (doubling time of healthy cells). All other indicators of the fitness of cell species are calculated by the ratio of the value of 1200 to the corresponding doubling time of the population of each particular species.

3. Model calibration for cancer and precancerous cell dynamics

To proceed with the equations of the model, we note that the abundance of nutrients in pancreas facilitates favorable conditions for both healthy, cancerous and precancerous cells. Until the very latest stages of the disease, the number of healthy pancreatic cells is in vast excess over the number of cancer cells. Therefore, we assume that the number of

Preprints (www.preprints.org) | NOT PEER-REVIEWED | Posted: 1 September 2022 doi:10.20944/preprints202209.0023.v1

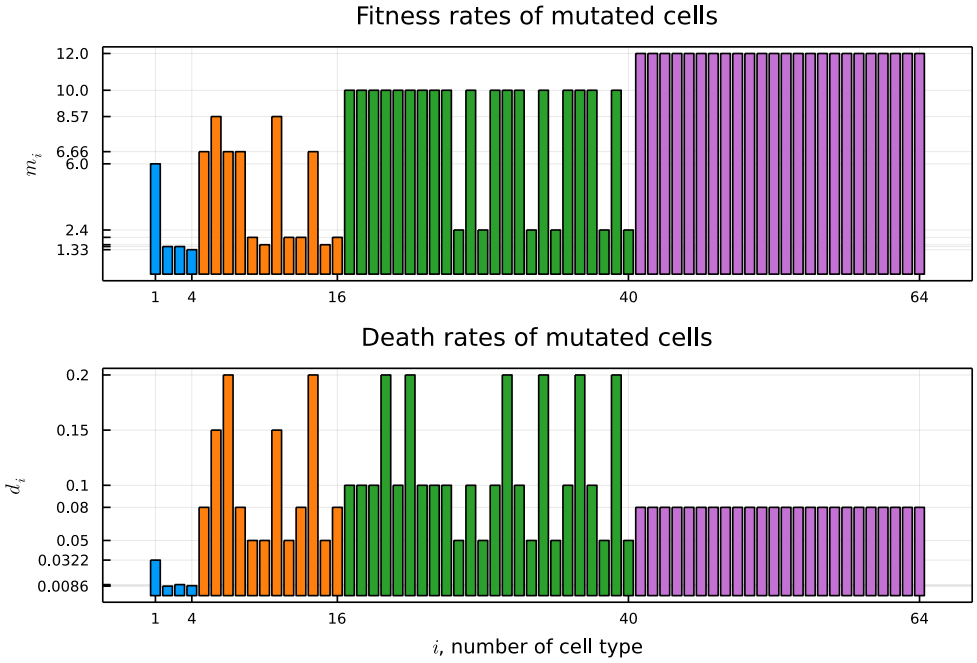

Figure 2. Fitness rates m_i and death rates d_i of mutated cells. Colors correspond to one-letter (blue), two-letter (orange), three-letter (green), four-letter (magenta) mutations.

healthy cells remains constant and the system of equations stated below describes only growth dynamics for cancerous and precancerous cells.

Let $\hat{S}$ be the upper limit of all cells in pancreas, $S_c(t)$ — number of cancerous and precancerous cells at time $t \geq 0$, $S_c(0) = 0$.

The supply of cells with nutrients is described by function $\psi(t)$, $t \geq 0$, which is the solution of the equation

$$\frac{d\psi(t)}{dt} = r\psi(t)\left(1 - \frac{\psi(t)}{K}\right), \quad \psi(0) = 10^{-5}, \tag{10}$$

where $K = 0.18$ (scaled with respect to the maximal value 1), $r = 0.00075$ day^{-1}.

The system of equations governing the populations dynamics of the number of cancerous and precancerous cells is given by

$$\frac{dv_i(t)}{dt} = (\psi(t) - S_c(t))\left(\hat{S}(QMv(t))_i + \gamma_i\right) - d_i v_i(t), \quad v_i(0) = 0, \quad i = 1, \ldots, 64. \tag{11}$$

Here $v_i(t)$ is the frequency of i-th cell type relative to $\hat{S}$, M — diagonal matrix of the fitness landscape $M = diag(m_1, m_2, \ldots, m_{64})$, d_i — the corresponding death rates. The constants γ_i^c $(i = 1, 2, \ldots, 64)$ characterize the effect of symbiosis between healthy cells and cancerous and precancerous cells of type i. The numerical values of constants γ_i^c are given in Table 3.

Let us denote the set of indices (numbers) of m-letter cells type as I_m $(m = 1, 2, 3, 4)$. Given the stated representation of elements of mutation matrix Q, we have

$$(QMv(t))_i = q_m \sigma_{i \in I_m} m_i v_i(t), \quad i \in I_m, \quad m = 1, 2, 3, 4. \tag{12}$$

Equation 10 implies that the average fitness of the system is given by

$$f(t) = (\psi(t) - S_c(t))^{-1} \tag{13}$$

The tumor cells expressing non-self antigens are eliminated by antitumor immune responses mediated by CD8+ T cells (CTL) [19]. However, during cancer progression, CTLs

Preprints (www.preprints.org) | NOT PEER-REVIEWED | Posted: 1 September 2022 doi:10.20944/preprints202209.0023.v1

Table 3. Estimates of the effect of symbiosis between healthy cells and cancerous and precancerous cells of type i.

Mutation type, i	K	P	C	S	KC	KS	KP	
Symbiosis, γ_i^c (10^5)	4	1	1	2	20	24	24	
Mutation type, i	PS	CP	CS	KCS	KPC	KPS	CPS	$KPCS$
Symbiosis, γ_i^c (10^5)	33	32	32	20	20	20	36	20

loss their function and acquire exhaustion state due to immunosuppression within the tumor micro-environment [19–21]. The system of equations accounting for interactions between cancerous and stromal cells leads and the effect of cancer antigen-induced CD8 T cell response $T(t)$ leads to the model system of ODEs presented below:

$$\frac{dv_i(t)}{dt} = (\psi(t) - S_c(t))(\widehat{S}(QMv(t))_i + \gamma_i^c) - d_i v_i(t) - \\ - \frac{\gamma_i v_i(t) T(t) \widehat{T}}{K_T + \beta(\widehat{S} S_c(t))^2 + \widehat{T} \cdot T(t)};\ v_i(0) = 0,\ i = 1,\ 2,\ ...,\ 64. \quad (14)$$

The last term in the above equation describes the T-cell mediated elimination of cancer cells depending on the functional state of the tumor-specific T cells.

The equation for cancer-specific CD8 T cells takes into account their homeostatic turnover, the cancer-antigens induction of their clonal expansion and the functional exhaustion taking place when the number of cancer cells increases above a certain threshold.

$$\frac{dT(t)}{dt} = \frac{T^*}{\widehat{T}} + b\frac{\widehat{S} \cdot S_c(t) T(t)}{\omega + \widehat{S}^2 (S_c(t))^2} - d_T T(t),\ T(0) = 0.3 \quad (15)$$

Hence, it is considered that positive and negative regulations determine the strength of the immune response. For a low or medium abundance of cancer cells the antiviral immune response is stimulated (the nominator expression). However, at high density of cancer cells it gets down-regulated (the denominator term). In particular, for high tumor cell density, the down-regulation of T cell activity takes place known as functional exhaustion). The description follows the frameworks suggested earlier for virus infections [22,23].

If the we take into account the immune cell-mediated elimination of the cancer cells, then the fitness if the system is defined by

$$f_{im}(t) = f(t)\frac{1}{1 + \frac{C(t)}{D(t)}}. \quad (16)$$

Here the functions $C(\cdot)$, $D(\cdot)$ are given by

$$C(t) = \frac{\hat{T} \cdot T(t) \cdot \sum_{i=1}^{64} \gamma_i v_i(t)}{K_T + \beta(\hat{S} \cdot S_c(t))^2 + \hat{T} \cdot T(t)}, \quad (17)$$

$$D(t) = \sum_{i=1}^{64} d_i v_i(t), \quad (18)$$

and $f(t)$ is the fitness of the system without the impact of the immune system.

Here, $\widehat{T} = 2.5 \cdot 10^5$ cells/ml refers to the homeostatic level of tumor-antigen-specific CTLs, $K_T = 10^3$ cells/ml estimates the CTL density for a half-maximal elimination rate of tumor cells, $T^* = 10^3$ cells/ml/day is the homeostatic supply, $\beta = 10^{-11}$ (cells/ml)^2, $b = 10$ day^{-1}, $\omega = 10^7$ (cells/ml)^2 stand for the down-regulation of the CTL effector function, the clonal proliferation rate of CTLs and the threshold for cancer cell abundance inducing functional exhaustion in CTLs. For simulations, we used a rescaled value of CTL with respect to their homeostatic abundance $\widehat{T}$.

Preprints (www.preprints.org) | NOT PEER-REVIEWED | Posted: 1 September 2022 doi:10.20944/preprints202209.0023.v1

4. Computational experiments

Figure 3 shows the results of numerical calculations of the system without taking into account the interaction with the cells of the immune system. It predicts the evolution of the abundance of the mutants determined by the differences in their fitness values. Cells bearing one mutations appear earlier and have their population size larger than that of the two-, three-, and four-mutation cells by a factor of ten.

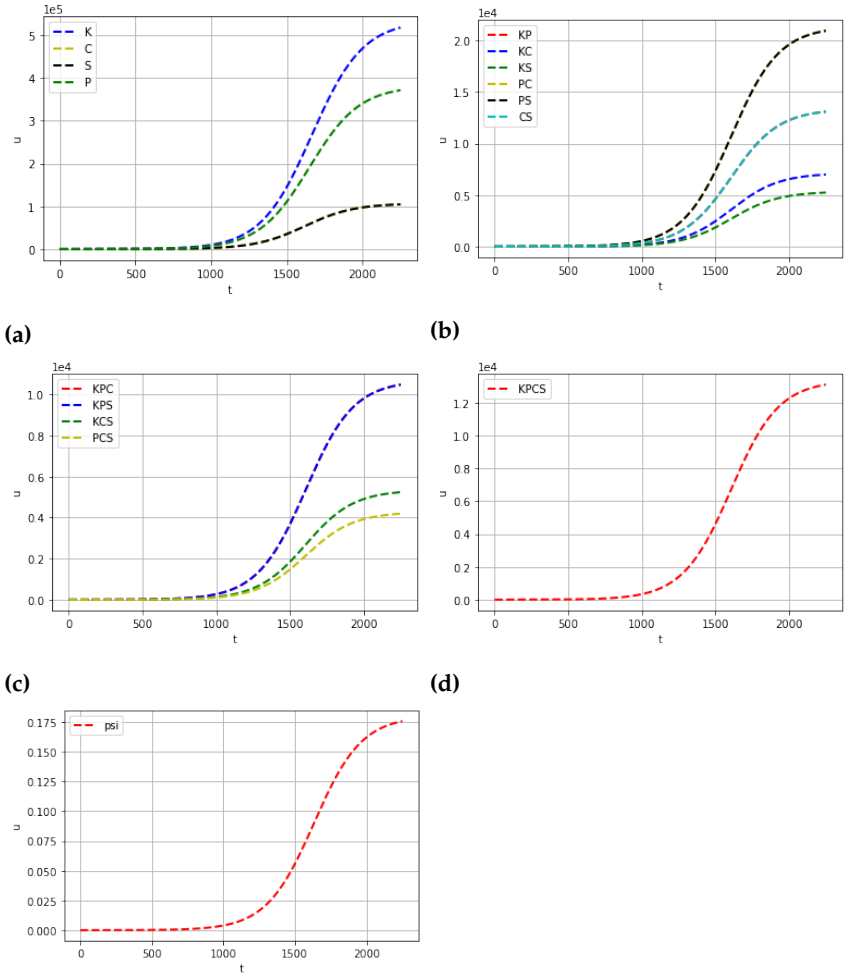

Figure 3. The dynamics of the populations of cancerous and precancerous cells without taking into account the effects of immune cells. The x-axis is the time in days. On the y-axis, the number of (quasispecies) nutated pancreatic cells. From left to right: a) single mutation cells, b) two mutation cells, c) three mutation cells, d) KPCS cells bearing four mutations. f) dynamics of nutrients intake.

Figure 4 shows the results of experiment taking into account the interaction of cancer cells with the effector CD8+ T cells of the immune system. The following graph shows the change in the total number of cancer cells under the influence of cells of the immune system. The CTL-mediated elimination of cancer cells slows down the emergence of the single- and double mutations cells. However, the CTL response fail to control the emergence and abundance tumor cells with three- and four mutations.

Preprints (www.preprints.org) | NOT PEER-REVIEWED | Posted: 1 September 2022 doi:10.20944/preprints202209.0023.v1

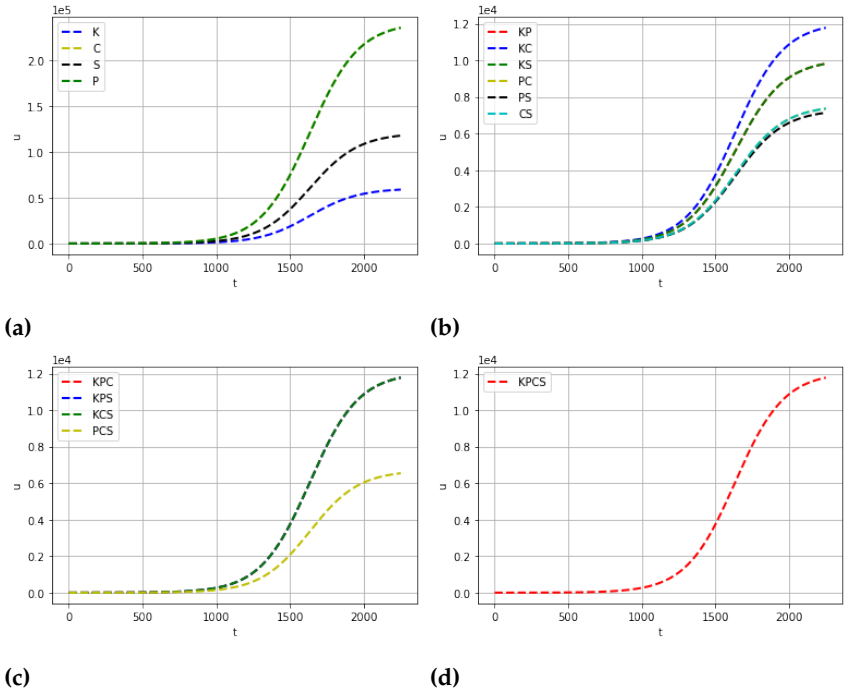

Figure 4. The dynamics of populations of cancerous and precancerous cells, taking into account the impact of effector CTLs of the immune system. a) One-mutation cells, b) two-mutation cells, c) three-mutation cells, d) KPCS cells.

The dynamics of the CTL response to tumor antigens is depicted in Figure 5. Initially, the appearance of non-self antigens expressed by tumor cells induces the clinal expansion of CTLs. However, when the density of cancer cells reaches a certain threshold, the immune response is down-regulated (daya 650) and the CTLs acquire a exhaustion phenotype.

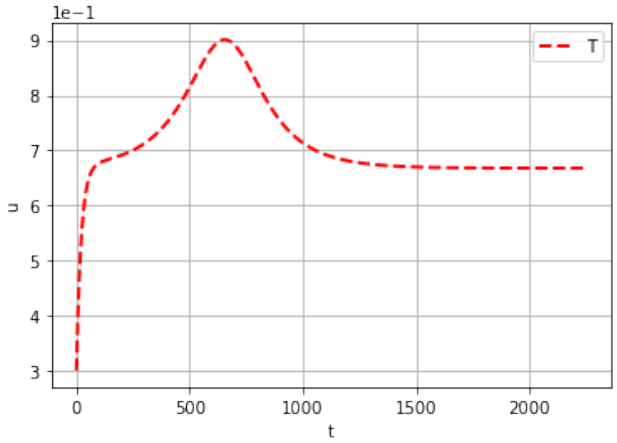

Figure 5. Dynamics of the anti-tumor CTL response. On the x-axis - time in days. On the y-axis - the relative number of cells on a scale of 10^4.

Finally, the model can be used to predict the evolution of the mean cancer call population fitness determining the rate of cancer progression. Figure 6 shows the dynamics of the mean fitness corresponding to uncontrolled growth of cancer cells and the effect of immune control which delays the emergence of more aggressive cancer quasispecies.

 doi:10.20944/preprints202209.0023.v1

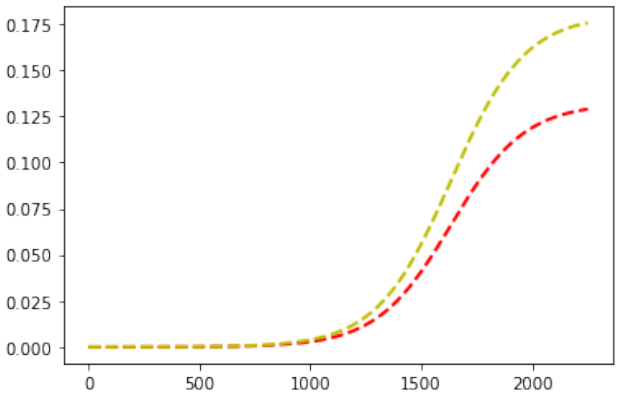

Figure 6. Mean system fitness growth of the cancer cell population without the effect of immune system (yellow line at the top) and taking into account the elimination of cancer cells by effector CTLs (red line at the bottom).

5. Conclusions

In this work, we developed a quantitative mathematical model of the evolutionary dynamics of pancreatic cancer cells. The model describes the emergence of cancer cells bearing different number of mutations as evolving quasispecies system consisting 64 subpopulations bearing one-, two-, three- and four mutations. In addition, the antitumor CTL response is taken into account. Further model development need to consider the relationship between the number of mutation and antigenicity of the respective cancer cells.

The empirical estimates of the doubling times and mortality rates are used to calibrate the model dynamics. The model consitently reproduces the sequential evolution of cancer cell populations. In provides an analytical tool to examine various approaches to the treatment of Pancreatic Ductal AdenoCarcinoma, including the chemotherapy, surgery, reinvigoration of exhausted CTLs and the CAR-T cell therapies [20,21,24,25].

Author Contributions: Conceptualization, A.B., N.L., D.Y. and G.B.; methodology, A.B., N.L., D.Y. and G.B.; software, M.C.; validation, A.B., N.L., and D.Y.; formal analysis, A.B., M.C.; investigation, A.B., N.L., M.C., D.Y., D.G. R.S. and G.B.; data curation, N.L.; writing—A.B., N.L., M.C., D.Y., D.G. R.S. and G.B.; writing—review and editing, A.B., N.L., M.C., D.Y., D.G. R.S. and G.B.; visualization, M.C., D.G., and R.S.; supervision, A.B.; funding acquisition, A.B., D.Y.. All authors have read and agreed to the published version of the manuscript.

Funding: The reported study was funded by RFBR and the Royal Society of London (RS), project number 21-51-10006. A.B. was supported by the Moscow Center for Fundamental and Applied Mathematics at Lomonosov Moscow State University (agreement with the Ministry of Education and Sciences of the Russian Federation No. 075-219-1621) and D.G., R.S. and G.B. were partly supported by the Moscow Center for Fundamental and Applied Mathematics at INM RAS (agreement with the Ministry of Education and Sciences of the Russian Federation No. 075-15-2022-286).

Data Availability Statement: Not applicable.

Conflicts of Interest: The authors declare no conflict of interest. The funders had no role in the design of the study; in the collection, analyses, or interpretation of data; in the writing of the manuscript, or in the decision to publish the results.

Abbreviations

The following abbreviations are used in this manuscript:

PDAC	Pancreatic Ductal AdenoCarcinoma
CTL	effector CD8+ T lymphocyte
ODE	ordinary differential equation

References

1. Kleeff, J.; Korc, M.; Apte, M.; La Vecchia, C.; Johnson, C.D.; Biankin, A.V.; Neale, R.E.; Tempero, M.; Tuveson, D.A.; Hruban, R.H.; et al. Pancreatic cancer. *Nature Reviews Disease Primers* **2016**, *2*, 16022. https://doi.org/10.1038/nrdp.2016.22.
2. Lu, J.; Yu, R.; Liu, R.; Liang, X.; Sun, J.; Zhang, H.; Wu, H.; Zhang, Z.; Shao, Y.W.; Guo, J.; et al. Genetic aberrations in Chinese pancreatic cancer patients and their association with anatomic location and disease outcomes. *Cancer Medicine* **2021**, *10*, 933–943. https://doi.org/10.1002/cam4.3679.
3. Zhou, B.; Xu, J.W.; Cheng, Y.G.; Gao, J.Y.; Hu, S.Y.; Wang, L.; Zhan, H.X. Early detection of pancreatic cancer: Where are we now and where are we going?: Early detection of pancreatic cancer. *International Journal of Cancer* **2017**, *141*, 231–241. https://doi.org/10.1002/ijc.30670.
4. Erkan, M.; Hausmann, S.; Michalski, C.W.; Fingerle, A.A.; Dobritz, M.; Kleeff, J.; Friess, H. The role of stroma in pancreatic cancer: diagnostic and therapeutic implications. *Nature Reviews Gastroenterology & Hepatology* **2012**, *9*, 454–467. https://doi.org/10.1038/nrgastro.2012.115.
5. Karamitopoulou, E. Tumour microenvironment of pancreatic cancer: immune landscape is dictated by molecular and histopathological features. *British Journal of Cancer* **2019**, *121*, 5–14. https://doi.org/10.1038/s41416-019-0479-5.
6. Louzoun, Y.; Xue, C.; Lesinski, G.B.; Friedman, A. A mathematical model for pancreatic cancer growth and treatments. *Journal of Theoretical Biology* **2014**, *351*, 74–82. https://doi.org/10.1016/j.jtbi.2014.02.028.
7. Gaspar, N.J.; Li, L.; Kapoun, A.M.; Medicherla, S.; Reddy, M.; Li, G.; O'Young, G.; Quon, D.; Henson, M.; Damm, D.L.; et al. Inhibition of Transforming Growth Factor β Signaling Reduces Pancreatic Adenocarcinoma Growth and Invasiveness. *Molecular Pharmacology* **2007**, *72*, 152–161. https://doi.org/10.1124/mol.106.029025.
8. Bachem, M.G.; Zhou, S.; Buck, K.; Schneiderhan, W.; Siech, M. Pancreatic stellate cells—role in pancreas cancer. *Langenbeck's Archives of Surgery* **2008**, *393*, 891–900. https://doi.org/10.1007/s00423-008-0279-5.
9. Mace, T.A.; Ameen, Z.; Collins, A.; Wojcik, S.; Mair, M.; Young, G.S.; Fuchs, J.R.; Eubank, T.D.; Frankel, W.L.; Bekaii-Saab, T.; et al. Pancreatic Cancer-Associated Stellate Cells Promote Differentiation of Myeloid-Derived Suppressor Cells in a STAT3-Dependent Manner. *Cancer Research* **2013**, *73*, 3007–3018. https://doi.org/10.1158/0008-5472.CAN-12-4601.
10. Makohon-Moore, A.; Iacobuzio-Donahue, C.A. Pancreatic cancer biology and genetics from an evolutionary perspective. *Nature Reviews Cancer* **2016**, *16*, 553–565. https://doi.org/10.1038/nrc.2016.66.
11. Yachida, S.; Iacobuzio-Donahue, C.A. Evolution and dynamics of pancreatic cancer progression. *Oncogene* **2013**, *32*, 5253–5260. https://doi.org/10.1038/onc.2013.29.
12. Hayashi, A.; Hong, J.; Iacobuzio-Donahue, C.A. The pancreatic cancer genome revisited. *Nature Reviews Gastroenterology & Hepatology* **2021**, *18*, 469–481. https://doi.org/10.1038/s41575-021-00463-z.
13. Makohon-Moore, A.P.; Zhang, M.; Reiter, J.G.; Bozic, I.; Allen, B.; Kundu, D.; Chatterjee, K.; Wong, F.; Jiao, Y.; Kohutek, Z.A.; et al. Limited heterogeneity of known driver gene mutations among the metastases of individual patients with pancreatic cancer. *Nature Genetics* **2017**, *49*, 358–366. https://doi.org/10.1038/ng.3764.
14. Yachida, S.; Jones, S.; Bozic, I.; Antal, T.; Leary, R.; Fu, B.; Kamiyama, M.; Hruban, R.H.; Eshleman, J.R.; Nowak, M.A.; et al. Distant metastasis occurs late during the genetic evolution of pancreatic cancer. *Nature* **2010**, *467*, 1114–1117. https://doi.org/10.1038/nature09515.
15. Notta, F.; Chan-Seng-Yue, M.; Lemire, M.; Li, Y.; Wilson, G.W.; Connor, A.A.; Denroche, R.E.; Liang, S.B.; Brown, A.M.K.; Kim, J.C.; et al. A renewed model of pancreatic cancer evolution based on genomic rearrangement patterns. *Nature* **2016**, *538*, 378–382. https://doi.org/10.1038/nature19823.
16. Yegorov, I.; Novozhilov, A.S.; Bratus, A.S. Open quasispecies models: Stability, optimization, and distributed extension. *Journal of Mathematical Analysis and Applications* **2020**, *481*, 123477. https://doi.org/10.1016/j.jmaa.2019.123477.
17. Li, Y.; He, Y.; Peng, J.; Su, Z.; Li, Z.; Zhang, B.; Ma, J.; Zhuo, M.; Zou, D.; Liu, X.; et al. Mutant Kras co-opts a proto-oncogenic enhancer network in inflammation-induced metaplastic progenitor cells to initiate pancreatic cancer. *Nature Cancer* **2021**, *2*, 49–65. https://doi.org/10.1038/s43018-020-00134-z.
18. Mayerle, J. Pancreatic cancer: why the cell of origin matters. *Nature Reviews Gastroenterology & Hepatology* **2022**, *19*, 279–279. https://doi.org/10.1038/s41575-022-00595-w.

19. Farhood, B.; Najafi, M.; Mortezaee, K. CD8 $^{+}$ cytotoxic T lymphocytes in cancer immunotherapy: A review. *Journal of Cellular Physiology* **2019**, *234*, 8509–8521. https://doi.org/10.1002/jcp.27782.
20. Bruni, D.; Angell, H.K.; Galon, J. The immune contexture and Immunoscore in cancer prognosis and therapeutic efficacy. *Nature Reviews Cancer* **2020**, *20*, 662–680. https://doi.org/10.1038/s41568-020-0285-7.
21. Mohamed, A.; Huang, Y.H. Life support for transitory exhausted CTLs. *Trends in Immunology* **2021**, *42*, 1057–1059. https://doi.org/10.1016/j.it.2021.10.012.
22. Bocharov, G. Modelling the Dynamics of LCMV Infection in Mice: Conventional and Exhaustive CTL Responses. *Journal of Theoretical Biology* **1998**, *192*, 283–308. https://doi.org/10.1006/jtbi.1997.0612.
23. Baral, S.; Antia, R.; Dixit, N.M. A dynamical motif comprising the interactions between antigens and CD8 T cells may underlie the outcomes of viral infections. *Proceedings of the National Academy of Sciences* **2019**, *116*, 17393–17398. https://doi.org/10.1073/pnas.1902178116.
24. Takano, S.; Fukasawa, M.; Shindo, H.; Takahashi, E.; Hirose, S.; Fukasawa, Y.; Kawakami, S.; Hayakawa, H.; Kuratomi, N.; Kadokura, M.; et al. Clinical significance of genetic alterations in endoscopically obtained pancreatic cancer specimens. *Cancer Medicine* **2021**, *10*, 1264–1274. https://doi.org/10.1002/cam4.3723.
25. Singhi, A.D.; George, B.; Greenbowe, J.R.; Chung, J.; Suh, J.; Maitra, A.; Klempner, S.J.; Hendifar, A.; Milind, J.M.; Golan, T.; et al. Real-Time Targeted Genome Profile Analysis of Pancreatic Ductal Adenocarcinomas Identifies Genetic Alterations That Might Be Targeted With Existing Drugs or Used as Biomarkers. *Gastroenterology* **2019**, *156*, 2242–2253.e4. https://doi.org/10.1053/j.gastro.2019.02.037.